Geophysica (2017), 52(1), 3–20

An Overview of Climate Variability in Finland During the Common Era

Samuli Helama

Natural Resources Institute Finland
P.O. Box 16, 96301 Rovaniemi, Finland

(Submitted: Dec 15, 2016; Accepted: May 22, 2017)

Abstract

Quantitative palaeoclimate estimates of past summer temperature and moisture (Palmer Drought Severity Index, PDSI) variability were derived from tree-ring based products of gridded reconstructions for the regions of Finland and the north-central Europe and southern Fennoscandia (CNCESF) where strong anomalies have previously been identified during the past millennium. The past climate variability in Finland was found to agree with several temperature and PDSI anomalies of annual to centurial duration as previously defined for the CNCESF. The long-term variations included the Medieval Climate Anomaly (MCA) from tenth to thirteenth centuries and the Little Ice Age (LIA) that preceded the 20th and 21st century positive trends in temperature and hydroclimate. The MCA was likely warm in both regions and less rainy especially in the CNCESF region. The LIA conditions were generally cold and variable according to hydroclimate reconstructions. Moreover, the temperature reconstructions indicated two-stage LIA with excursions of warm climates during the first halves of the 15th and 16th centuries. The MCA drought was followed by dry spells during the mid-15th century and at the turn of the eighteenth to nineteenth centuries especially in the CNCESF region and during the World War II in Finland. These variations could be putatively related to changes in the proxy-based indications of the North Atlantic origin, the North Atlantic Oscillation and the Atlantic Multidecadal Oscillation, in addition to the solar forcing. Among the coldest summers, the years of 800, 1453, 1821 and 1601 could be related to volcanic forcing. In general, the correlations between the reconstructed anomalies between the two regions were higher for temperature than PDSI; the magnitude of inter-annual climate fluctuations exceeded those of low-frequency variations whereas the correlations between the reconstructed time-series were higher the lower the frequencies under investigation. Although much can be learned from the existing reconstructions, more proxy data is needed to unravel the spatial and temporal details of climate anomalies beyond the era of instrumental observations.

Keywords: Medieval Climate Anomaly, Little Ice Age, tree-ring, temperature, drought

1 Introduction

Climate variability can be inferred back in time beyond the era of modern meteorological observations using proxy archives. Considering the relative shortness of meteorological time-series, typically spanning no more than the past 100–200 years (*Vose et al.*, 1992; *Heino*, 1994), the proxy data commonly constitutes the only source of information available for understanding the past climatic changes and variations on timescales of centuries and millennia. Studying these variations is important for several reasons. Analyses of proxy data help to increase our understanding of climate variations in the long course of time and to assess the climate models of future climate scenarios (*Bradley*, 2000; *Braconnot* et al., 2012). In palaeoclimatology, the primary sources of infor-

mation originate from indirect estimates of past climate that are climate-sensitive records of geological, glaciological or palaeontological records or historical archives (*Bradley*, 1999).

Probably the most commonly used temporally high-resolution proxy data originates from tree rings (*Fritts*, 1976; *Briffa*, 2000; *Hughes*, 2011). Compared to other proxy types, the primary benefit of tree-ring records is that is this data is precisely dated to exact calendar years. Moreover, the process of dating a high number of individual series to calculate a mean chronology substantially enhances the climate signal in resulting chronology. The site of tree growth determines which factors may affect the growth. Near the altitudinal and latitudinal treelines tree growth variability is commonly limited by temperature of the growing season. At lower altitudes and latitudes the growth becomes increasingly controlled by moisture conditions. Moreover, it is important that chronologies are selected according to statistics indicating their potential for climatic reconstructions. The strength of the climatic signal in tree-ring data is enhanced and the extent of non-climatic and local factors reduced when tree-ring chronologies of several sites are averaged and/or by extracting the signal from a large set of data using principal component analysis (*Fritts*, 1976, 1991). Thus, the mean chronologies and their networks are calibrated and verified against the instrumental climate records (*Briffa et al.*, 2001; *D'Arrigo et al.*, 2006; *Wilson et al.*, 2016). As a result, the tree-ring data can be statistically transformed into the estimates of climate variability as originally observed at the weather stations.

In Europe, the ongoing progress of collecting and analysing tree-ring materials and data has enabled construction of several chronologies spanning over the past millennium and even the Common Era. These chronologies are constructed from tree-ring materials not only from living trees but those of historical buildings, archaeological excavations, and remains of ancient wood preserved over centuries and millennia as subfossils in anoxic conditions in peatland and lake sediments. In the regions where a specific climatic factor limits the growth, these chronologies may constitute palaeoclimate proxy data for reconstructing the climatic changes and variations over much of the late Holocene. Moreover, the networks of such data form the basis for gridded high-resolution climate reconstruction over wide areas. Recently, the datasets combining tree rings of biological, historical, archaeological and paleoontological origin have been used to reconstruct year-to-year maps of summer warmth, coldness, wetness, and dryness over Europe and the Mediterranean Basin during the Common Era (*Cook et al.*, 2015; *Luterbacher et al.*, 2016). A number of tree-ring chronologies from Finland contribute to these gridded reconstructions, the palaeoclimate value of those data being previously proved on local and regional scale (*Helama et al.*, 2009a, 2009b; *Esper et al.*, 2012; *Matskovsky and Helama*, 2014, 2016).

The main aim of this study is to illustrate the climate variability in Finland during the Common Era (i.e. the Anno Domini era). The reconstructions examined in this study originate from recent tree-ring based analyses of European climate variability (*Cook et al.*, 2015; *Luterbacher et al.*, 2016). The estimates of past temperature and moisture (Palmer Drought Severity Index) conditions are extracted from the gridded datasets for

representations of climate variability in Finland and compared with reconstructions made for central Europe. These reconstructions characterise the long-term climate features during the putative 'Medieval Climate Anomaly' (*Diaz et al.*, 2011; *Graham et al.*, 2011) and 'Little Ice Age' (*Bradley and Jones*, 1993; *Matthews and Briffa*, 2005), and help to place the ongoing climatic trends in a long-term context. In so doing this study illustrates the value of tree rings as palaeoclimate proxy data on different spatial and temporal scales and demonstrates the importance of this kind of reconstructions to better understand the variability in our changing climate.

2 Palaeoclimate datasets

Annually-resolved gridded summer temperature fields over Europe were originally reconstructed using a network of nine tree-ring chronologies around the continent (see *Luterbacher et al.*, 2016 and references therein). Only chronologies containing a strong temperature signal and spanning at least over past 700 years were selected, their locations encompassing the region from 41° to 68° N and from 1° to 25° E. Land-only temperature grid (5° × 5°) spanning the period 1850–2010 (*Jones et al.*, 2012) was for used for statistically transforming (*Tingley and Huybers*, 2010) the data of tree-ring chronologies into palaeoclimate estimates for 61 grid points. The mean temperature history over Finland was acquired here from 60° to 70° N and from 20° to 30° E. As for the PDSI fields, another tree-ring dataset has been developed from a network of altogether 106 moisture-sensitive tree-ring chronologies around Europe, North Africa and the Levant (see *Cook et al.*, 2015 and references therein). The chronologies were selected for their target signal and the gridded PDSI fields (0.5° × 0.5°) spanning over the region were produced by statistically calibrating (*Cook et al.*, 1999) the data of tree-ring chronologies against the instrumentally based PDSI data (1901–1978) available on identical resolution (*van der Schrier et al.*, 2013). The mean PDSI history over Finland was excerpted from the data of 5414 grid points to represent hydroclimate variations from 60° to 70° N and from 20° to 30° E. Strong anomalies in the gridded PDSI data were previously observed over a region of continental north-central Europe and southern Fennoscandia (CNCESF) (from 50° to 60° N and from 5° to 20° E) (*Cook et al.*, 2015). In this study, the PDSI history in Finland was compared with corresponding variations over the CNCESF region. Comparisons were likewise made between the temperature histories over Finland and the CNCESF region.

3 Reconstructed temperature variability

Reconstructed temperatures demonstrated markedly fluctuating climatic conditions since 755 CE (Fig. 1). There appeared a rise in summer temperatures since the 1920s, this change characterising the modern period. Explained by a linear trend, the warming over the past 100 years (1911–2010) was evident at an overall rate of 0.09 °C decade $^{-1}$ in the CNCESF region and 0.05 °C decade $^{-1}$ in Finland. While these indications reproduce, in general, the findings of climatic warming in these regions (*Tuomen-*

virta and Heino, 1996; *Tietäväinen et al.*, 2010; *Jones et al.,* 2012; *Mikkonen et al.*, 2015), the palaeoclimate data additionally place the most recent changes in a context of long-term temperature variability. With these regards, much colder temperatures were evident over the 13th through 19th centuries, this climatic phase overlapping with the timing of the Little Ice Age (LIA). As for the initiation of the LIA, there are suggestions of both the earlier (ca. 1300) and later (ca. 1570) years (*Matthews and Briffa*, 2005), both of them appearing reasonable in the context of these temperature reconstructions. That is, the LIA appeared a multi-centennial period during which the temperatures prevailed notably below the 20th century level, with exceptions of annual-to-decadal events of transiently warmer climate. Such exceptions occurred in these reconstructions especially during the first halves of the 15th and 16th centuries (Fig. 1a). The LIA would thus follow a two-stage model, this feature making it elusive to judge between its possible 13th or 16th century starts. Predating the LIA, a long period with warm temperatures occurred from late 9th through 12th centuries. The warmth of this period may have been interrupted only with some annual to multi-annual events, in addition to cold decades during the early 12th century. Both the duration and timing of this climatic period are comparable with those of the Medieval Climate Anomaly (MCA) during which relatively warm temperature conditions have likely prevailed particularly over the North Atlantic sector and to some extent on hemispheric scales. With these regards, it has been suggested that the MCA have likely prevailed between AD 900–1400 (*Diaz et al.*, 2011; *Graham et al.*, 2011). The reconstructions examined here (Fig. 1) appeared indicative of somewhat earlier end of the MCA-related warm conditions in both regions, especially in Finland.

These fluctuations characterised the summer temperature variations both in Finland and in the CNCESF region. Calculating Pearson correlation between the centennial temperature variations (black lines in Fig. 1) confirmed this correspondence with $r = 0.811$ (755–2010). Temperature levels comparable to the recent warming were evident during the MCA. The reconstructions for Finland and the CNCESF region exhibited warmest centennial periods for 915–1014 and 912–1011, respectively, with temperatures very similar to their recent levels. Moreover, the CNCESF reconstruction indicated temperatures around 0.3 °C warmer over the 1130–1229 period than over the 1911–2010 period. Such warm MCA conditions were not found for Finland, where temperatures may have remained roughly at the 20th century mean level. The coldest temperatures were observed for Finland during the 1251–1350 period (0.8 °C below the 20th century level), as opposed to the CNCESF temperatures reaching their minimum level over the 1576–1675 period (0.7 °C below that level). During the latter period low temperatures were evident also for Finland. Temperature differences between the two regions were more obvious on shorter temporal scales. Correlations between the multi-decadal (dark grey lines in Fig. 1) and decadal (medium grey lines in Fig. 1) temperature variations were however relatively high with $r = 0.791$ and $r = 0.736$, respectively.

Compared to low-frequency temperature variability, the annual temperature values (light grey lines in Fig. 1) indicated somewhat lower correspondence between the two regions with $r = 0.680$ (755–2010). The warmest years were dominated by the 20th

century estimates (Table 1a). In the CNCESF region five out of ten warmest years were found between the latest two decades (1991–2005), as opposed to Finland where the 1930s was represented by two very warm years (1936 and 1937) and by two years (1997 and 2002) at the turn of the millennium. Individual markedly warm summers were found also during the LIA. Such events occurred in 1831 in Finland and in 1859 and 1868 in the CNCESF region. Individual markedly cold years were experienced also during the 12th and 17th centuries (Table 1b), these estimates indicating the recurrence of cold events both during the warm (i.e. MCA) and the cold (i.e. LIA) climatic periods. The cold summer in 1902 was the only representative of the 20th century estimates in these lists.

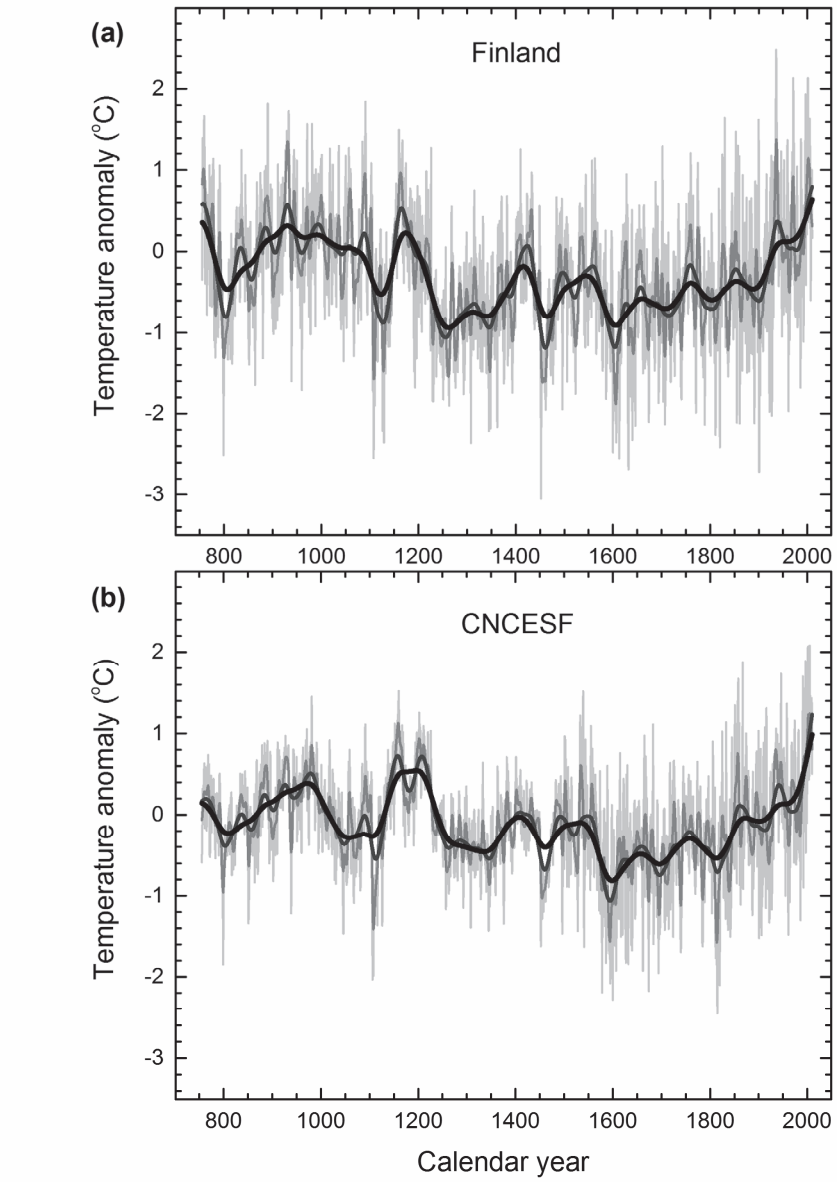

Fig. 1. Temperature variability since 755 CE reconstructed for June through August season in Finland (a) and the CNCESF region (b) (*Luterbacher et al.*, 2016). Variations are shown with respect to 1901-2000 period as inter-annual (light grey line), decadal (medium grey line), multi-decadal (dark grey line) and centennial (black line) time scales.

4 Reconstructed PDSI variability

The two PDSI reconstructions were more divergent than the temperature reconstructions (Fig. 2). Moreover, the PDSI evidence for the MCA and LIA appeared less obvious. These differences were quantified by Pearson correlations calculated between the two PDSI reconstructions with r = -0.081, r = 0.055, r = -0.002, and r = 0.038 for centennial, multi-decadal, decadal, and annual variations, respectively. It is notable that the PDSI is driven by precipitation anomalies, antecedent atmospheric conditions, and soil characteristics (*Guttman*, 1998). Spatial heterogeneity in these variables likely contributes to this dissimilarity. Comparing the two PDSI reconstructions over the 1000–2012 period revealed considerably higher correspondence in their variations with r = 0.329, r = 0.284, r = 0.182, and r = 0.160 as calculated for centennial, multi-decadal, decadal, and annual variations, respectively. These correlations were indicative of potentially decreasing common signal in the proxy data over the earlier times.

Despite these dissimilarities, the two reconstructions portrayed several periods of coinciding drought events in Finland and in the CNCESF region. First, the long-term drought of the 1000–1200 period, overlapping with the MCA, was highlighted for the CNCESF region (*Cook et al*., 2015) and was, albeit to a lesser degree, a long dry period also in Finland (*Helama et al*., 2009a). Similar drought was nevertheless indicated here especially during the 10th and 11th centuries (Fig. 2). Second, a drought of the mid-15th century from 1437 to 1473 and a third similar event from 1779 to 1827 (*Cook et al.*, 2015) were present in not only in CNCESF region but also in Finland, and punctuated the reconstructed PDSI variability as distinct negative anomalies. Over the recent decades, the PDSI appeared increasingly positive as reconstructed especially for the CNCESF region. This trend was consistent with the observed increase in regional summer precipitation (*Yiou and Cattiaux*, 2013).

Apart from the foregoing droughts, the two reconstructions exhibited coinciding multi-annual hydroclimatic events recorded as pluvials during the 1130s and 1730s (Fig. 2). The extent of these events was reflected in the list of most positive PDSI estimates, found for Finland in 1137 and 1138 and for the CNCESF region in 1140 and 1734/1738 (Table 1c). However, it is notable that the lists of pluvial and drought extremes did not contain common single-year events (Table 1d). Moreover, the drought recorded in 1940 was among the driest years in Finland, this event remaining as the only representative of the 20th and 21st century estimates. Interestingly, this year overlapped with the World War II drought known to have prevailed in the region during the Continuation War (*Kuusisto*, 2004). Observational evidence has shown that this drought spanned over the 4-year period from 1939 to 1942 (*Hydrografinen toimisto*, 1944, 1948). Compared to these past events, the recent dry years appeared less anomalous. Over the past 25 years the only exception was the PDSI value for Finland in 2006. This year obtained a reconstructed value as low as -2.4 and as such exceeding the level of one standard deviation (1.7). In fact, the drought of 2006 is known to have contributed not only to reduced tree growth but increased tree mortality in the same region (*Helama et al.,* 2016).

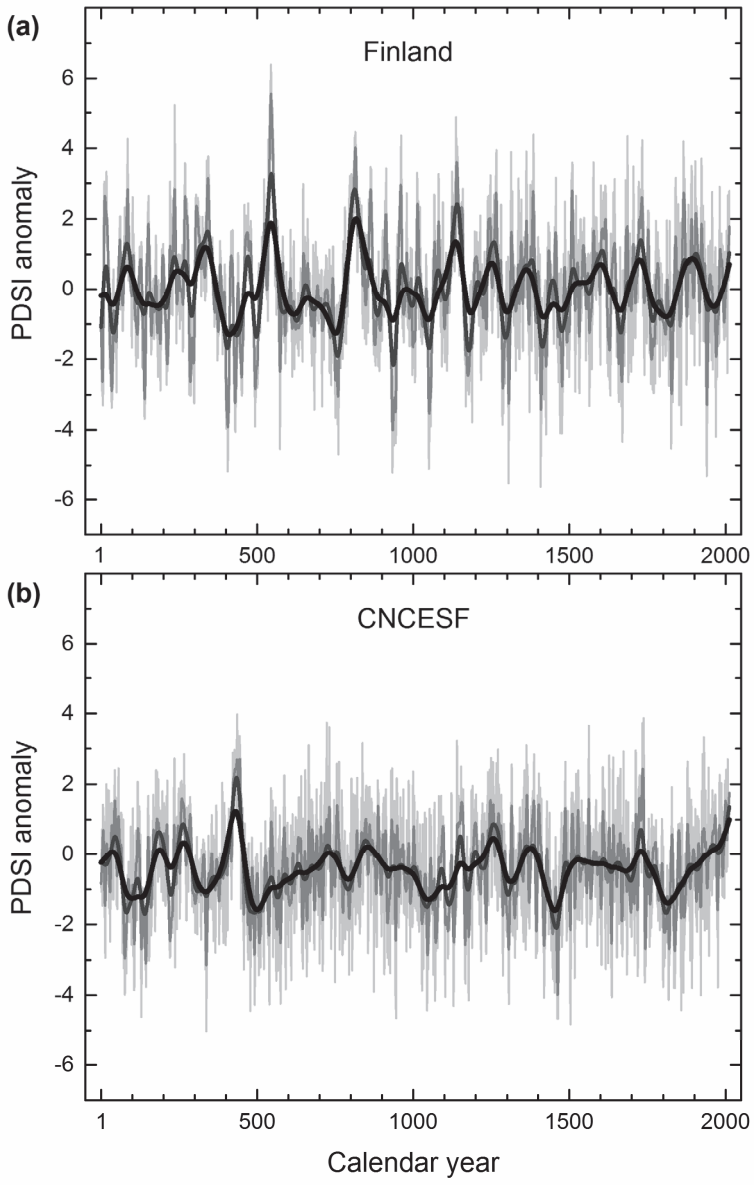

Fig. 2. Moisture variability since 1 CE reconstructed as Palmer Drought Severity Index (PDSI) for June through August season in Finland (a) and the CNCESF region (b) (*Cook et al.*, 2015). Variations are shown as inter-annual (light grey line), decadal (medium grey line), multi-decadal (dark grey line) and centennial (black line) time scales.

Table 1. The years with the most positive and negative anomalies (with respect to 1901-2000 period) in temperature (ΔT, °C) (a, b) and Palmer Drought Severity Index (ΔPDSI, index) (c, d) reconstructed for Finland and in the CNCESF region over the 755-2010 period.

(a)	Year	ΔT Finland	Year	ΔT CNCESF	(b)	Year	ΔT Finland	Year	ΔT CNCESF
	1937	2.5	2006	2.1		1453	-3.1	1816	-2.5
	1972	2.1	2003	2.1		1902	-2.7	1601	-2.3
	2002	2.1	2002	2.1		1633	-2.7	1579	-2.2
	1997	1.9	1997	1.9		1614	-2.6	1675	-2.2
	1092	1.8	1868	1.9		1109	-2.5	1821	-2.1
	891	1.8	1947	1.7		800	-2.5	1596	-2.1
	1936	1.8	1992	1.7		1601	-2.5	1107	-2.0
	934	1.7	1859	1.7		1821	-2.4	1109	-2.0
	760	1.7	1161	1.5		1309	-2.4	1695	-2.0
	1831	1.6	1540	1.5		1130	-2.4	1108	-1.9
(c)	Year	ΔPDSI Finland	Year	ΔPDSI CNCESF	(d)	Year	ΔPDSI Finland	Year	ΔPDSI CNCESF
	1137	5.2	1738	3.7		934	-4.9	1503	-5.0
	961	5.1	1734	3.5		1408	-4.8	1461	-4.9
	1903	5.0	1562	3.4		933	-4.7	1464	-4.9
	1680	4.8	1931	3.1		1305	-4.6	945	-4.9
	812	4.8	1140	3.0		760	-4.6	1462	-4.7
	815	4.6	837	2.9		1940	-4.2	1044	-4.7
	1313	4.6	1362	2.9		757	-4.0	1858	-4.6
	1363	4.5	1271	2.8		1826	-4.0	943	-4.6
	1138	4.4	1712	2.7		1306	-3.8	1129	-4.5
	1892	4.4	1673	2.7		935	-3.8	1306	-4.5

5 Potential forcing factors

Climatic variations in both regions are influenced by the proximity of the North Atlantic Ocean. In this context, the North Atlantic Oscillation (NAO; *Hurrell*, 1995) is a frequently suggested driver of regional climate variability and change over these regions as signified by both the instrumentally based (*Hurrell*, 1995; *Folland et al.*, 2009) and the proxy-based (*Trouet et al.*, 2009; *Wassenburg et al.*, 2013; *Baker et al.*, 2015; *Ortega et al.*, 2015; *Faust et al.,* 2016) NAO-indices (Fig. 3). First, the NAO-index describes the oscillation of atmospheric masses producing large-scale changes in the mean wind speed and direction over the North Atlantic with significant effects on temperature and precipitation (*Hurrell*, 1995; *Folland et al.*, 2009). These effects materialise also in the regions under this investigation (*Tuomenvirta et al.*, 2001; *Helama and Holopainen*, 2012). Second, there may have been long-term variations between the predominantly positive and negative NAO phases overlapping with the MCA and LIA intervals (*Trouet et al.*, 2009), respectively. It is notable that for summer season, the positive (negative) NAO-phase is associated with generally warmer (colder) and less (more) rainy conditions largely over the studied regions (*Folland et al.*, 2009). Thus, the positive NAO-

phase during the MCA (*Trouet et al.*, 2009) could explain the generally warmer and drier conditions as indeed reconstructed for Finland and the CNCESF region, whereas the negative NAO-phase could likewise explain the colder and moister conditions during the following centuries (*Luoto and Helama*, 2010). Recently, the persistently positive NAO phase during the MCA has however been questioned (*Ortega et al.*, 2015). Yet, additional proxy evidence has been presented in support of the change from generally positive NAO phase during the MCA towards negative phase during the LIA (*Wassenburg et al.*, 2013; *Baker et al.*, 2015). This view generally agreed also with the NAO-reconstruction based on the Norwegian fjord sediments (*Faust et al.,* 2016). Apart from the positive NAO phase during the 11th and 12th centuries, there is no general agreement between the NAO reconstructions nor between the NAO and temperature/PDSI reconstructions (Fig. 3).

Over the recent past, there has been a decline in summer NAO index, since the 1990s (*Hanna et al.*, 2015). Moreover, especially in the PDSI reconstruction of the CNCESF region demonstrate a considerable recent wetting, consistent with precipitation data showing a positive trend in summer precipitation over the northern Europe (50°N-70°N, 8°W-35°E), as observed by Yiou and Cattiaux (2013) for the 1971–2012 period. Considering the negative association between the summer NAO-index and the moisture over the region (*Folland et al.*, 2009), it cannot be ruled out that the recent trend in summer moisture is at least partly NAO-related. However, recent analyses have shown that the trends in European precipitation can be more strongly attributed to changes in large-scale synoptic circulation than to changes in the NAO-index (*Hoy et al.,* 2014; *Fleig et al.,* 2015), especially in June and August. Synoptic types mainly representative of westerlies have significantly increased since 1960s, especially in June (*Fleig et al.,* 2015). Consistent with these findings, the westerly winds bring more rain onto the northern part of Europe, especially around the Baltic Sea (*Hoy et al*., 2014).

Apart from the circulation patterns of purely atmospheric origin, an important measure of North Atlantic variability is determined by the Atlantic Multidecadal Oscillation (AMO), defined as the detrended, smoothed mean sea surface temperatures over the region 0°N to 60°N and 75°W to 7.5°W (*Enfield et al.*, 2001). Considering the AMO connections to continental climate (*Sutton and Hodson*, 2005), and the role of thermohaline circulation (THC) in driving the AMO (*Delworth and Mann*, 2000), the North Atlantic sedimentary records sensitive to THC could potentially be used to explain the low-frequency palaeoclimate variations. Temperature reconstructions (Fig. 3) are compared with a palaeoceanographic record indicative of the speed of deep ocean flow (Iceland–Scotland Overflow Water), an important component of the THC (*Bianchi and McCave*, 1999). The phases of increased flow speed coincided both with the MCA and the mid-LIA warming (the first half of the 15th century), the phases of lower speed being coeval with the cool period of the LIA. Possibly, the high-latitude North Atlantic plays a role behind the continental climate variability as generally suggested (*Bianchi and McCave*, 1999) and previously demonstrated using Finnish tree-ring data (*Helama et al.*, 2009b). Moreover, the trends of warming over the 20th and 21st centuries were evident in both temperature reconstructions. Among natural forcings, both the high solar

irradiance and low volcanic aerosol loading may have contributed to recent high-latitude climate warming (*Overpeck et al.*, 1997). Also the AMO index illustrates a strong positive trend in the Atlantic sea surface temperatures since the 1970s, with implication that the AMO may have contributed to recent European summer warming (*Sutton and Hodson*, 2005). Moreover, the palaeoceanographic reconstructions indicate that the recent enhancement of heat transfer to North Atlantic is unprecedented over the past 2000 years (*Spielhagen et al.*, 2011). Likely, the 20th and 21st century changes in the AMO may have resulted from natural multi-decadal climate variability in addition to anthropogenic forcing (*Ting et al.*, 2014).

Solar variability is a frequently suggested external forcing that may conceivably explain the past climate variations, with possible connections to the NAO (*Gray et al.*, 2010). The negative NAO phases coinciding the times of quieter Sun during the Wolf (1280–1340), Spörer (1420–1530) and Maunder (1645–1715) minima, as already recorded by Eddy (1983), have recently been demonstrated (*Faust et al.*, 2016). Similar connections were recorded as coinciding cold periods in both of the temperature reconstructions (Fig. 3), when compared with the reconstructions of the total solar irradiance derived from cosmogenic radionuclide ^{10}Be measured in ice cores (*Steinhilber et al.*, 2009). In Finland, these findings add to previous indications of low summer temperatures as reconstructed particularly during the late Maunder minimum (*Helama et al.,* 2014). According to models, the lower NAO-index during the periods of reduced solar activity could result from the corresponding change in sea surface temperatures, with atmospheric-hydrological feedbacks, this NAO response further modifying the downstream air temperature anomalies in Europe (*Shindell et al.*, 2001). Similar pathways of solar signal may also have operated on longer scales. Previous comparisons have indicated that variations in Sun's activity could explain, at least partially, the warmer MCA and colder LIA (*Helama et al.*, 2010). At the same time, these suggestions would indicate that solar forcing cannot alone explain the full variance of climate change evident in the proxy records but remains as only one factor among others.

On shorter scales, the forcing by volcanic aerosols following the explosive eruptions has been used to explain the annual to multi-annual temperature fluctuations evident in documentary and proxy records of climate variability (*Briffa et al.*, 1998; *Fischer et al.*, 2007; *Helama et al.*, 2013). Large eruptions constitute climatic forcing when their sulphate aerosol emissions reach the stratosphere and reduce solar irradiance on Earth, leading to post-eruptive cooling of summer temperatures at global scale (*Robock*, 2000). Consistent volcanic signals were apparent as negative temperature anomalies in 1821 and 1601 in both regions, in 1453 and 800 in Finland, and in 1695 and 1108 in the CNCESF region (Table 1b), these events coinciding with the years of increased estimates of global volcanic forcing as derived from the recently compiled bipolar ice-core timescales and sulphur records (*Sigl. et al.*, 2015). Moreover, the negative temperature anomalies in 1109 in Finland and in 1816 in the CNCESF region appeared to postdate the ice-core events of volcanic forcing in 1108 and 1815 (Tambora eruption) by one

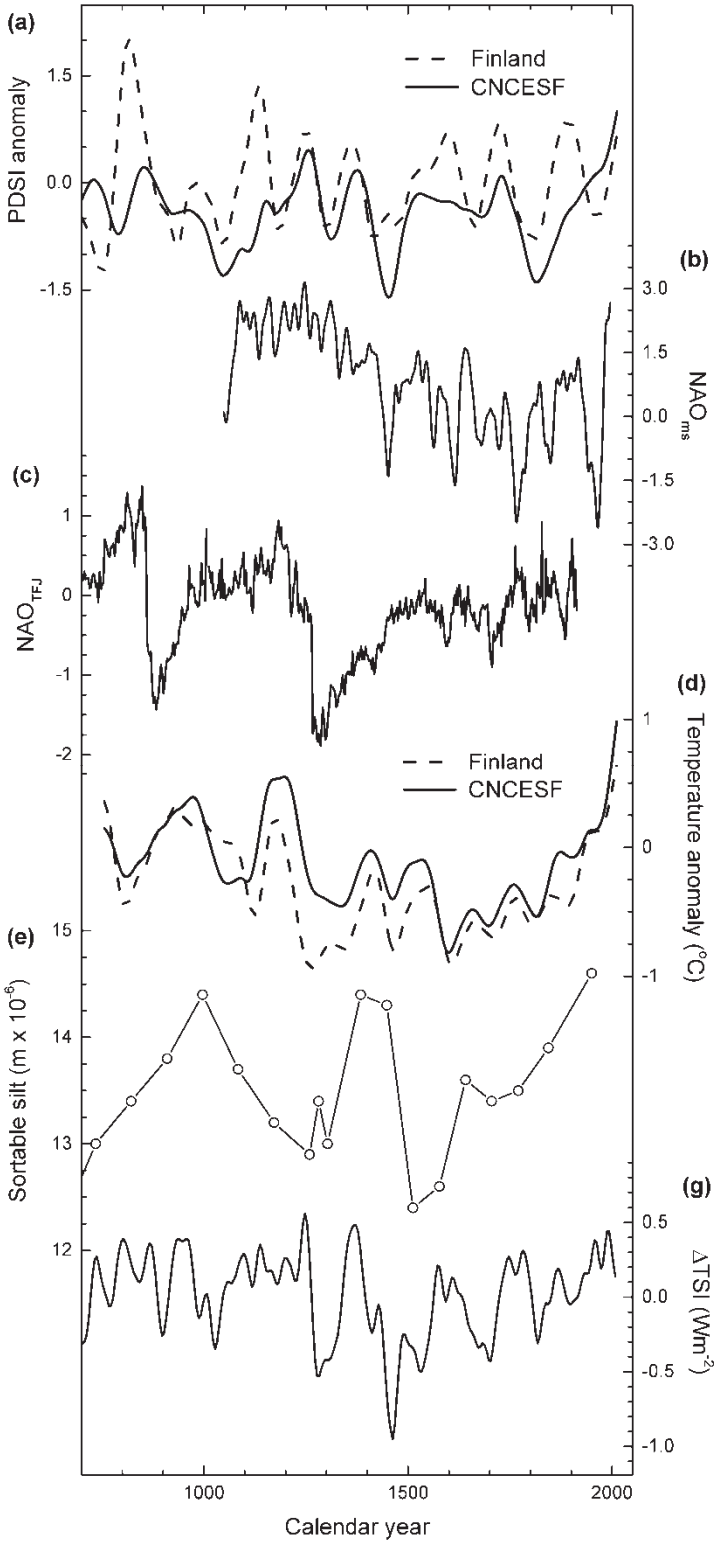

Fig. 3. Records of climate variability and its forcing factors presented as the reconstructions of (a) the Drought Severity Index (PDSI) for June through August season (*Cook et al.*, 2015), (b) the North Atlantic Oscillation based on tree-ring/speleothem records (NAO_{ms}) (*Trouet et al.*, 2009) and (c) fjord sediments (NAO_{TFJ}) (*Faust et al.*, 2016), (d) the temperature for June through August season (*Luterbacher et al.*, 2016), (e) the speed of deep ocean flow (Iceland–Scotland Overflow Water) indicated by sortable silt mean size (10-63mm) (*Bianchi and McCave*, 1999), and (f) the ice-core derived solar forcing as total solar irradiance (ΔTSI) (*Steinhilber et al.*, 2009).

year, suggesting a possible connection with delayed response. In fact, a 3-year period from 1107 to 1109 appeared anomalously cold in the CNCESF region. Likely, there have been a number of volcanic summers with less intensive cooling in the two regions (e.g. *Fischer et al.*, 2007). Their examination would require more exhaustive analyses and remained beyond the scope of this work.

6 Discussion and conclusions

Climatic fluctuations during the Common Era are subtle in amplitude in comparison to those of glacial times; however, there is a need for detailed insightful knowledge of their dynamical behaviour for evaluating the magnitude and effects of ongoing changes in our climate (*Eronen and Zetterberg*, 1996). Palaeoclimatology helps us to understand the current state of climate in a similar way the human history helps us to understand the modern society and puts it in a perspective.

This paper has focussed on tree-ring based reconstructions of past climate variability. In fact, the dendroclimatic methods applied to climate-sensitive tree-ring datasets are seen as an ideal proxy to reconstruct calendar year dated short-to-long timescale climate variations (*Helama et al.* 2017). Despite the progress in chronology construction, the underlying proxy network of tree-ring data is still far from ideal. The future palaeoclimate reconstructions should benefit from a higher number of tree-ring series and mean chronologies. Such reconstructions will detail the spatial characteristics of the temperature and hydrological anomalies in Europe and adjacent areas.

Here, the data of reconstructed climate variability were characteristically similar to instrumental data (e.g. *Heino,* 1994) in several ways. Correlations between the regions were higher for low-frequency, rather than high-frequency variability, and for temperature rather than moisture variability. Moreover, the magnitude of inter-annual variations greatly exceeded the strength of long-term trends. Temperature and PDSI anomalies for the previously defined CNCESF region (*Cook et al.*, 2015; *Luterbacher et al.*, 2016) and were not fully comparable to anomalies in obtained for Finland.

The reconstructions for these regions did however illustrate a long-term climate evolution with conditions identifiable as the MCA and LIA, and agreed reasonably about the recent trends observed for temperature and moisture in northern Europe. Climate variability is commonly attributed to the solar and volcanic forcing, with additional influence of the North Atlantic variability, including the NAO and AMO. Tree-ring evidence of this study has demonstrated that similar factors have possibly played a role in shaping the climate variability in Finland during the Common Era. These factors come with expected contributions to our future climate and are likely to modify the trajectories driven by greenhouse forcing.

Acknowledgements

Paul Krusic is thanked for a code extracting sets of data from products of gridded temperature reconstructions and Kimmo Ruosteenoja for his comments on an earlier version of this manuscript. The manuscript was written while the author was supported by Grant 288267 from the Academy of Finland.

References

Baker, A., J.C. Hellstrom, B.F.J. Kelly, G. Mariethoz and V. Trouet, 2015. A composite annual-resolution stalagmite record of North Atlantic climate over the last three millennia, *Sci. Rep.* **5**, 10307.

Bianchi, G.G. and I.N. McCave, 1999. Holocene periodicity in North Atlantic climate and deep-ocean flow south of Iceland, *Nature* **397**, 515–517.

Bradley, R.S., 1999. *Paleoclimatology: reconstructing climates of the Quaternary*. International Geophysics Series **Vol. 64**, Academic Press, London.

Bradley, R.S., 2000. Past global changes and their significance for the future, *Quat. Sci. Rev.* **19**, 391–402.

Bradley, R.S. and P.D. Jones, 1993. 'Little Ice Age' summer temperature variations: their nature and relevance to recent global warming trends, *Holocene* **3,** 367–376.

Braconnot, P., S.P. Harrison, M. Kageyama, P.J. Bartlein, V. Masson-Delmotte, A. Abe-Ouchi, B. Otto-Bliesner and Y. Zhao, 2012. Evaluation of climate models using palaeoclimatic data, *Nature Clim. Change* **2**, 417–424.

Briffa, K.R., 2000. Annual climate variability in the Holocene: interpreting the message of ancient trees, *Quat. Sci. Rev.* **19**, 87–105.

Briffa, K.R., P.D. Jones, F.H. Schweingruber and T.J. Osborn, 1998. Influence of volcanic eruptions on Northern Hemisphere summer temperature over the past 600 years, *Nature* **393,** 450–455.

Briffa, K.R., T.J. Osborn, F.H. Schweingruber, I.C. Harris, P.D. Jones, S.G. Shiyatov and E. Vaganov, 2001. Low-frequency temperature variations from a northern tree ring density network, *J. Geophys. Res.* **106**, 2929–2941.

Cook, E.R., D.M. Meko, D.W. Stahle and M.K. Cleaveland, 1999. Drought reconstructions for the continental United States, *J. Climate* **12**, 1145–1162.

Cook, E.R., R. Seager, Y. Kushnir, K.R. Briffa, U. Büntgen, D. Frank, P.J. Krusic, W. Tegel, G. van der Schrier, L. Andreu-Hayles, M. Baillie, C. Baittinger, N. Bleicher, N. Bonde, D. Brown, M. Carrer, R. Cooper, K. Čufar, C. Dittmar, J. Esper, C. Griggs, B. Gunnarson, B. Günther, E. Gutierrez, K. Haneca, S. Helama, F. Herzig, K.-U. Heussner, J. Hofmann, P. Janda, R. Kontic, N. Köse, T. Kyncl, T. Levanič, H. Linderholm, S. Manning, T.M. Melvin, D. Miles, B. Neuwirth, K. Nicolussi, P. Nola, M. Panayotov, I. Popa, A. Rothe, K. Seftigen, A. Seim, H. Svarva, M. Svoboda, T. Thun, M. Timonen, R. Touchan, V. Trotsiuk, V. Trouet, F. Walder, T. Ważny, R. Wilson and C. Zang, 2015. Old World megadroughts and pluvials during the Common Era, *Science Advances* **1**, e1500561.

D'Arrigo, R., R. Wilson and G. Jacoby, 2006. On the long-term context for late twentieth century warming, *J. Geophys. Res.* **111**, D03103.

Delworth, T.L. and M.E. Mann, 2000. Observed and simulated multidecadal variability in the Northern Hemisphere, *Clim. Dyn.* **16**, 661–676.

Diaz, H.F., R. Trigo, M.K. Hughes, M.E. Mann, E. Xoplaki and D. Barriopedro, 2011. Spatial and temporal characteristics of climate in medieval times revisited, *Bull. Am. Meteorol. Soc.* **92**, 1487–1500.

Eddy, J.A., 1983. The Maunder minimum: a reappraisal, *Solar Physics* **89,** 195–207.

Enfield, D.B., A.M. Mestas-Nuñez and P.J. Trimble, 2001. The Atlantic multidecadal oscillation and its relation to rainfall and river flows in the continental U.S., *Geohys. Res. Lett.* **28,** 2077–2080.

Eronen, M. and P. Zetterberg, 1996. Climatic changes in northern Europe since late glacial times, with special reference to dndroclimatological studies in northern Finnish Lapland, *Geophysica* **32**, 35–60.

Esper, J., D.C. Frank, M. Timonen, E. Zorita, R.J.S. Wilson, J. Luterbacher, S. Holzkämper, N. Fischer, S. Wagner, D. Nievergelt, A. Verstege and U. Büntgen, 2012. Orbital forcing of treering data, *Nature Clim. Change* **2**, 862–866.

Faust, J.C., K. Fabian, G. Milzer, J. Giraudeau and J. Knies, 2016. Norwegian fjord sediments reveal NAO related winter temperature and precipitation changes of the past 2800 years, *Earth Planet. Sci. Lett.* **435**, 84–93.

Fischer, E.M., J. Luterbacher, E. Zorita, S.F.B. Tett, C. Casty and H. Wanner, 2007. European climate response to tropical volcanic eruptions over the last half millennium, *Geophys. Res. Lett.* **34,** L05707.

Fleig, A.K., L.M. Tallaksen, P. James, H. Hisdal and K. Stahl, 2015. Attribution of European precipitation and temperature trends to changes in synoptic circulation, *Hydrol. Earth Syst. Sci.* **19,** 3093–3107.

Folland, C.K., J. Knight, H.W. Linderholm, D. Fereday, S. Ineson and J.W. Hurrell 2009. The summer North Atlantic Oscillation: past, present, and future, *J. Clim.* **22,** 1082–1103.

Fritts, H.C., 1976. *Tree rings and climate*, Academic Press, New York.

Fritts, H.C., 1991. *Reconstructing large-scale climatic patterns from tree-ring data*, The University of Arizona Press, Tucson.

Graham, N.E., C.M. Ammann, D. Fleitmann, K.M. Cobb and J. Luterbacher, 2011. Support for global climate reorganization during the "Medieval Climate Anomaly", *Clim. Dyn.* **37**, 1217–1245.

Gray, L.J., J. Beer, M. Geller, J.D. Haigh, M. Lockwood, K. Matthes, U. Cubasch, D. Fleitmann, G. Harrison, L. Hood, J. Luterbacher, G.A. Meehl, D. Shindell, B. van Geel and W. White, 2010. Solar influences on climate, *Rev. Geophys.* **48,** RG4001.

Guttman, N.B., 1998. Comparing the Palmer Drought Index and the Standardized Precipitation Index. *J. Am. Water Resources Ass.* **34**, 113–121.

Hanna, E., T.E. Cropper, P.D. Jones, A.A. Scaife and R. Allan, 2015. Recent seasonal asymmetric changes in the NAO (a marked summer decline and increased winter variability) and associated changes in the AO and Greenland Blocking Index, *Int. J. Climatol.* **35,** 2540–2554.

Heino, R., 1994. Climate in Finland During the Period of Meteorological Observations, *Finnish Meteorological Institute Contributions* **12**, 1–209.

Helama, S. and J. Holopainen, 2012. Spring temperature variability relative to the North Atlantic Oscillation and sunspots – A correlation analysis with a Monte Carlo implementation, *Palaeogeogr. Palaeoclim.* **326–328**, 128–134.

Helama, S., J. Holopainen, M. Macias-Fauria, M. Timonen and K. Mielikäinen, 2013. A chronology of climatic downturns through the mid- and late-Holocene: tracing the distant effects of explosive eruptions from palaeoclimatic and historical evidence in northern Europe, *Polar Research* **32,** 15866.

Helama, S., M. Macias Fauria, K. Mielikäinen, M. Timonen and M. Eronen, 2010. Sub-Milankovitch solar forcing of past climates: mid and late Holocene perspectives, *GSA Bull.* **122,** 1981–1988.

Helama, S., T.M. Melvin and K.R. Briffa, 2017. Regional curve standardization: State of the art, *Holocene* DOI: 10.1177/0959683616652709.

Helama, S., J. Meriläinen and H. Tuomenvirta, 2009a. Multicentennial megadrought in northern Europe coincided with a global El Niño–Southern Oscillation drought pattern during the Medieval Climate Anomaly, *Geology* **37**, 175–178.

Helama, S., K. Sohar, A. Läänelaid, H.M. Mäkelä and J. Raisio, 2016. Oak decline as illustrated through plant–climate interactions near the northern edge of species range, *Bot. Rev.* **82,** 1–23.

Helama, S., M. Timonen, J. Holopainen, M.G. Ogurtsov, K. Mielikäinen, M. Eronen, M. Lindholm and J. Meriläinen, 2009b. Summer temperature variations in Lapland during the Medieval Warm Period and the Little Ice Age relative to natural instability of thermohaline circulation on multi-decadal and multi-centennial scales, *J. Quaternary Sci.* **24,** 450–456.

Helama, S., M. Vartiainen, J. Holopainen, H.M. Mäkelä, T. Kolström and J. Meriläinen, 2014. A palaeotemperature record for the Finnish Lakeland based on microdensitometric variations in tree rings, *Geochronometria* **41,** 265–277.

Hoy, A., A. Schucknecht, M. Sepp and J. Matschullat, 2014. Large-scale synoptic types and their impact on European precipitation, *Theor. Appl. Climatol.* **116,** 19–35.

Hughes, M.K., 2011. Dendroclimatology in high-resolution paleoclimatology. In: Hughes, H.K., Swetnam, T.W. and Diaz, H.F. (eds), *Dendroclimatology. Progress and prospects.* Developments in Paleoenvironmental Research **Vol. 11**, Springer, Dordrecht.

Hurrell, J.W., 1995. Decadal trends in the North Atlantic Oscillation: regional temperatures and precipitation, *Science* **269**, 676–679.

Hydrografinen toimisto, 1944. *Vuosikirja 12 Årsbok 1937–1940*, Valtioneuvoston kirjapaino, Helsinki.

Hydrografinen toimisto, 1948. *Vuosikirja 13 Årsbok 1941–1945*, Valtioneuvoston kirjapaino, Helsinki.

Jones, P.D., D.H. Lister, T.J. Osborn, C. Harpham, M. Salmon and C.P. Morice, 2012. Hemispheric and large-scale land-surface air temperature variations: an extensive revision and an update to 2010, *J. Geophys. Res.* **117**, D05127.

Kuusisto, E., 2004. Kuvaus 1940-luvun poikkeuksellisesta kuivuudesta, *Finn. Environ.* **731**, 48.

Luoto, T.P. and S. Helama, 2010. Palaeoclimatological and palaeolimnological records from fossil midges and tree-rings: the role of the North Atlantic Oscillation in eastern Finland through the Medieval Climate Anomaly and Little Ice Age, *Quaternary Sci. Rev.* **29,** 2411–2423.

Luterbacher, J., J.P. Werner, J.E. Smerdon, L. Fernández-Donado, F.J. Gonzalez-Rouco, D. Barriopedro, F.C. Ljungqvist, U. Büntgen, E. Zorita, S. Wagner, J. Esper, D. McCarroll, A. Toreti, D. Frank, J.H. Jungclaus, M. Barriendos, C. Bertolin, O. Bothe, R. Brázdil, D. Camuffo, P. Dobrovolný, M. Gagen, E. García-Bustamante, Q. Ge, J.J. Gómez-Navarro, J. Guiot, Z. Hao, G.C. Hegerl, K. Holmgren, V.V. Klimenko, J. Martín-Chivelet, C. Pfister, N. Roberts, A. Schindler, A. Schurer, O. Solomina, L. von Gunten, E. Wahl, H. Wanner, O. Wetter, E. Xoplaki, N. Yuan, D. Zanchettin, H. Zhang and C. Zerefos, 2016. European summer temperatures since Roman times, *Environ. Res. Lett.* **11**, 024001, doi:10.1088/1748-9326/11/2/024001.

Matskovsky, V.V. and S. Helama, 2014. Testing long-term summer temperature reconstruction based on maximum density chronologies obtained by reanalysis of tree-ring data sets from northernmost Sweden and Finland, *Clim. Past* **10**, 1473–1487.

Matskovsky, V.V. and S. Helama, 2016. Direct transformation of tree-ring measurements into palaeoclimate reconstructions in three-dimensional space, *Holocene* **26**, 439–449.

Matthews, J.A. and K.R. Briffa, 2005. The 'Little Ice Age': re-evaluation of an evolving concept, *Geogr. Ann.* **87A**, 17–36.

Mikkonen, S., M. Laine, H.M. Mäkelä, H. Gregow, H. Tuomenvirta, M. Lahtinen and A. Laaksonen, 2015. Trends in the average temperature in Finland, 1847–2013, *Stoch. Environ. Res. Risk Assess.* 29, 1521–1529.

Ortega, P., F. Lehner, D. Swingedouw, V. Masson-Delmotte, C.C. Raible, M. Casado and P. Yiou, 2015. A model-tested North Atlantic Oscillation reconstruction for the past millennium, *Nature* **523**, 71–74.

Overpeck, J., Hughen, K., Hardy, D., Bradley, R., Case, R., Douglas, M., Finney, B., Gajewski, K.,

Jacoby, G., A. Jennings, S. Lamoureux, A. Lasca, G. McDonald, J. Moore, M. Retelle, S. Smith, A. Wolfe and G. Zielinski, 1997. Arctic environmental change of the last four centuries, *Science* **278**, 1251–1256.

Robock, A., 2000. Volcanic eruptions and climate, *Rev. Geophys.* **38,** 191–219.

Shindell, D.T., G.A. Schmidt, M.E. Mann, D. Rind and A. Waple, 2001. Solar forcing of regional climate change during the Maunder Minimum, *Science* **294,** 2149–2152.

Sigl, M., M. Winstrup, J.R. McConnell, K.C. Welten, G. Plunkett, F. Ludlow, U. Büntgen, M. Caffee, N. Chellman, D. Dahl-Jensen, H. Fischer, S. Kipfstuhl, C. Kostick, O.J. Maselli, F. Mekhaldi, R. Mulvaney, R. Muscheler, D.R. Pasteris, J.R. Pilcher, M. Salzer, S. Schüpbach, J.P. Steffensen, B.M. Vinther, T.E. Woodruff, 2015. Timing and climate forcing of volcanic eruptions for the past 2,500 years, *Nature* **523,** 543–549.

Spielhagen, R.F., K. Werner, S.A. Sørensen, K. Zamelczyk, E. Kandiano, G. Budeus, K. Husum, T.M. Marchitto and M. Hald, 2011. Enhanced modern heat transfer to the Arctic by warm Atlantic Water, *Science* **331**, 450–453.

Steinhilber, F., J. Beer and C. Fröhlich, 2009. Total solar irradiance during the Holocene, *Geophys. Res. Lett.* **36**, L19704.

Sutton, R.T. and D.L.R. Hodson, 2005. Atlantic Ocean forcing of North American and European summer climate, *Science* **309,** 115–118.

Tietäväinen, H., H. Tuomenvirta and A. Venäläinen, 2010. Annual and seasonal mean temperatures in Finland during the last 160 years based on gridded temperature data. *Int. J. Climatol.* **30**, 2247–2256.

Ting, M., Y. Kushnir and C. Li, 2014. North Atlantic Multidecadal SST Oscillation: External forcing versus internal variability, *J. Mar. Syst.* **133,** 27–38.

Tingley, M.P. and P. Huybers, 2010. A Bayesian algorithm for reconstructing climate anomalies in space and time: I. Development and applications to paleoclimate reconstructions problems, *J. Climate* **23**, 2759–2781.

Trouet, V., J. Esper, N.E. Graham, A. Baker, J.D. Scourse and D.C. Frank, 2009. Persistent positive North Atlantic Oscillation Mode dominated the Medieval Climate Anomaly, *Science* **324,** 78–80.

Tuomenvirta, H. and R. Heino, 1996. Climatic changes in Finland – Recent findings, *Geophysica* **32**, 61–75.

Tuomenvirta, H., H. Alexandersson, A. Drebs, P. Frich and P.O. Nordli, 2000. Trends in Nordic and Arctic temperature extremes and ranges, *J. Clim.* **13**, 977–990.

van der Schrier, G., J. Barichivich, K.R. Briffa and P.D. Jones, 2013. A scPDSI-based global data set of dry and wet spells for 1901–2009, *J. Geophys. Res.* **118**, 4025–4048.

Vose, R.S., R.L. Schmoyer, P.M. Steurer, T.C. Peterson, R. Heim, T.R. Karl and J. Eischeid, 1992. *The Global Historical Climatology Network: Long-term monthly temperature, precipitation, sea level pressure, and station pressure data*. Technical Report ORNL/CDIAC-53, NDP-041, Carbon Dioxide Information Analysis Center. Oak Ridge National Laboratory, Oak Ridge.

Wassenburg, J.A., A. Immenhauser, D.K. Richter, A. Niedermayr, S. Riechelmann, J. Fietzke, D. Scholz, K.P. Jochum, J. Fohlmeister, A. Schröder-Ritzrau, A. Sabaoui, D.F.C. Riechelmann, L. Schneider and J. Esper, 2013. Moroccan speleothem and tree ring records suggest a variable positive state of the North Atlantic Oscillation during the Medieval Warm Period, *Earth Planet. Sci. Lett.* **375**, 291–302.

Wilson, R., K. Anchukaitis, K.R. Briffa, U. Büntgen, E. Cook, R. D'Arrigo, N. Davi, J. Esper, D. Frank, B. Gunnarson, G. Hegerl, S. Helama, S. Klesse, P.J. Krusic, H.W. Linderholm, V. Myglan, T.J. Osborn, M. Rydval, L. Schneider, A. Schurer, G. Wiles, P. Zhang and E. Zorita, 2016. Last millennium northern hemisphere summer temperatures from tree rings: Part I: The long term context, *Quat. Sci. Rev.* **134**, 1–18.

Yiou, P. and J. Cattiaux, 2013. Contribution of atmospheric circulation to wet north European summer precipitation of 2012, *Bull. Am. Meteorol. Soc.* **94**, S39–S41.

Appendix

Year	Finland	CNCESF
755	0,69	-0,03
756	-0,35	-0,59
757	1,40	-0,25
758	1,29	0,33
759	0,64	0,18
760	1,67	0,41
761	1,26	0,63
762	-0,39	-0,16
763	0,86	0,31
764	0,64	0,58
765	0,30	0,25
766	-0,78	-0,19
767	0,47	0,17
768	0,70	0,39
769	0,26	0,74
770	-0,21	0,47
771	1,06	0,62
772	-0,66	-0,50
773	0,25	-0,52
774	0,83	0,29
775	0,91	0,48
776	-0,68	-0,22
777	0,76	0,23
778	1,01	0,34
779	1,14	0,21
780	0,69	0,44
781	-1,10	0,08
782	-0,67	-0,01
783	-1,31	-0,35
784	-1,06	-0,54
785	-0,21	0,26
786	-0,48	-0,08
787	-0,01	0,27
788	-0,88	-0,25
789	-1,06	-0,35
790	0,75	0,18
791	-0,33	-0,50
792	1,05	0,49
793	0,69	0,51
794	-0,37	0,13
795	-0,85	0,00
796	-0,66	-0,44
797	-1,03	-0,71
798	-0,43	-0,48
799	-0,91	-1,04
800	-2,51	-1,85
801	-0,97	-0,64
802	-1,12	-0,49
803	-1,28	-0,65

804	-0,83	-0,13
805	-1,03	-0,37
806	-0,99	-0,43
807	-0,80	-0,51
808	-1,02	-0,40
809	-1,34	-0,50
810	-0,82	-0,16
811	-0,10	0,02
812	-0,62	0,04
813	-0,39	0,12
814	-1,33	-0,49
815	-0,66	-0,40
816	0,22	0,22
817	-0,68	0,28
818	-1,39	-0,75
819	-0,77	-0,33
820	0,04	-0,41
821	-0,11	-0,68
822	-0,38	-0,40
823	-0,30	-0,24
824	-0,79	-0,63
825	0,13	-0,09
826	0,37	-0,26
827	0,54	-0,10
828	0,11	0,12
829	0,12	0,03
830	0,27	0,00
831	-0,13	-0,20
832	0,33	-0,02
833	0,54	0,18
834	-0,62	-0,15
835	0,58	0,51
836	-0,07	0,18
837	1,24	0,39
838	0,22	0,08
839	0,54	0,50
840	-0,31	-0,01
841	-0,09	-0,14
842	0,11	0,36
843	0,05	0,02
844	-0,61	-0,24
845	0,94	0,54
846	-0,21	-0,06
847	-0,14	0,26
848	-0,48	0,05
849	0,03	0,12
850	0,28	0,34
851	-0,93	-0,54
852	-1,29	-1,34
853	-1,40	-1,10
854	-0,48	-0,55
855	0,37	0,03

856	-0,16	0,10
857	-0,69	-0,33
858	-0,70	0,02
859	-0,61	-0,46
860	-0,26	-0,06
861	-0,94	-0,51
862	-0,62	-0,31
863	-0,62	-0,28
864	0,04	0,26
865	-1,65	-0,84
866	-0,59	-0,29
867	-0,20	-0,06
868	0,40	0,41
869	0,85	0,67
870	-0,27	-0,60
871	0,33	-0,74
872	-0,30	-0,68
873	0,30	-0,16
874	-0,07	0,29
875	0,46	0,52
876	0,96	0,53
877	-0,25	-0,26
878	0,76	0,62
879	-0,03	0,41
880	0,61	0,86
881	-1,32	-0,14
882	0,14	0,32
883	0,45	0,18
884	0,12	0,31
885	0,99	0,88
886	0,93	0,68
887	1,05	0,54
888	-0,21	0,32
889	0,24	0,69
890	0,93	0,72
891	1,82	0,91
892	-0,19	-0,05
893	0,35	0,30
894	0,50	-0,03
895	0,26	-0,60
896	0,16	-0,35
897	0,82	0,77
898	0,03	-0,05
899	0,77	-0,08
900	-0,82	-0,44
901	-0,51	-0,24
902	-0,98	-0,31
903	-1,02	-0,82
904	0,02	0,16
905	0,01	-0,01
906	0,23	0,04
907	-0,96	-0,50

908	-0,02	0,34
909	-0,07	-0,04
910	-0,56	-0,44
911	-0,85	-0,49
912	1,07	0,89
913	-0,17	0,18
914	-0,67	0,18
915	0,66	0,80
916	0,20	0,63
917	-0,50	0,09
918	-0,04	0,15
919	0,82	0,54
920	0,35	0,09
921	-0,52	0,09
922	0,91	0,67
923	-0,05	0,06
924	0,83	0,68
925	0,50	0,45
926	0,82	0,82
927	0,01	0,31
928	1,25	0,97
929	1,04	0,75
930	1,49	0,64
931	1,02	0,57
932	1,37	0,57
933	1,32	0,75
934	1,73	0,85
935	1,19	0,48
936	0,37	0,26
937	0,18	0,12
938	-0,31	-0,29
939	0,38	-0,33
940	-1,60	-1,22
941	-0,19	-0,15
942	0,00	-0,41
943	0,15	-0,31
944	1,06	0,80
945	1,24	0,79
946	1,03	0,57
947	0,68	0,08
948	-0,18	0,43
949	-0,10	0,37
950	-0,11	0,23
951	1,11	0,71
952	-0,44	-0,33
953	-0,06	-0,07
954	-0,43	0,00
955	-0,02	0,43
956	-0,34	0,43
957	0,24	0,51
958	-0,95	-0,17
959	0,17	0,27

960	0,33	0,50
961	-1,71	-0,47
962	0,01	0,27
963	0,24	0,31
964	0,78	0,83
965	-0,51	0,48
966	-0,62	0,23
967	0,02	0,38
968	-0,29	0,48
969	0,52	0,59
970	0,06	0,91
971	0,69	0,71
972	1,57	1,05
973	0,45	0,05
974	-0,41	0,13
975	0,20	0,19
976	-0,80	-0,37
977	0,31	0,56
978	0,71	0,84
979	-1,02	0,33
980	-0,09	0,65
981	-0,20	0,73
982	1,57	1,45
983	0,87	0,86
984	0,07	0,58
985	-0,26	0,26
986	0,94	0,77
987	0,49	0,56
988	0,05	0,49
989	-0,93	-0,18
990	1,00	0,65
991	0,09	0,35
992	0,53	0,89
993	0,15	0,78
994	0,33	0,12
995	0,95	0,51
996	0,04	-0,48
997	0,67	0,04
998	0,13	0,21
999	0,18	-0,14
1000	1,14	0,11
1001	0,74	0,00
1002	1,18	0,61
1003	0,22	-0,12
1004	0,14	-0,46
1005	0,10	0,23
1006	0,59	0,22
1007	0,31	-0,04
1008	-0,84	0,31
1009	0,10	0,43
1010	-0,22	-0,31
1011	0,39	0,03

1012	-0,18	-0,36
1013	-0,53	-0,30
1014	-0,35	-0,28
1015	-0,47	0,27
1016	-0,19	-0,19
1017	-0,78	-0,43
1018	0,56	0,51
1019	1,26	0,92
1020	0,78	0,11
1021	0,46	-0,09
1022	-0,05	-0,15
1023	-0,65	-0,32
1024	-0,32	-0,49
1025	1,06	0,56
1026	-0,11	0,33
1027	-0,02	0,10
1028	0,28	0,39
1029	-0,26	-0,81
1030	0,41	-0,01
1031	-0,32	0,18
1032	-0,68	-0,86
1033	0,46	0,06
1034	0,34	-0,53
1035	-0,05	-0,27
1036	0,15	-0,35
1037	1,30	0,33
1038	0,24	0,10
1039	0,32	0,26
1040	0,30	-0,53
1041	-0,80	-0,38
1042	-0,96	-0,63
1043	-0,65	-0,62
1044	-0,29	0,28
1045	-0,35	-0,36
1046	-0,37	-0,97
1047	-1,36	-1,47
1048	0,54	-0,56
1049	-0,05	-0,29
1050	-0,78	-0,18
1051	1,17	-0,35
1052	0,69	-0,37
1053	-0,94	-0,82
1054	-0,06	-0,87
1055	-0,11	-0,78
1056	0,05	-0,72
1057	0,75	0,04
1058	1,27	0,65
1059	0,17	0,32
1060	0,82	0,80
1061	1,01	0,12
1062	0,94	-0,27
1063	-0,14	-0,73

1064	0,52	0,15
1065	0,35	0,20
1066	0,14	0,21
1067	-0,51	-0,41
1068	-1,29	-0,99
1069	-1,03	-1,09
1070	-0,41	0,10
1071	0,01	-0,14
1072	-0,26	-0,77
1073	-0,23	-0,63
1074	-0,32	-0,72
1075	-0,52	-0,29
1076	-0,27	-0,41
1077	-0,89	-0,55
1078	-0,43	-0,04
1079	0,52	0,06
1080	0,51	-0,15
1081	-0,08	-0,59
1082	-0,53	-0,94
1083	-0,84	-0,84
1084	0,37	0,27
1085	-0,03	0,06
1086	1,36	0,63
1087	0,58	0,37
1088	0,60	-0,23
1089	0,53	-0,06
1090	0,58	-0,25
1091	1,20	0,51
1092	1,85	1,11
1093	0,62	0,51
1094	0,47	0,66
1095	-0,64	-0,05
1096	-0,77	-0,24
1097	0,42	0,53
1098	-0,01	-0,14
1099	-0,23	-0,10
1100	-0,28	-0,10
1101	0,21	0,07
1102	0,44	0,36
1103	0,60	0,28
1104	1,08	0,37
1105	0,50	0,53
1106	0,68	0,15
1107	-1,71	-2,03
1108	-1,62	-1,94
1109	-2,55	-1,99
1110	-1,39	-0,76
1111	-1,90	-1,16
1112	-0,87	-0,93
1113	-0,07	-1,04
1114	0,04	-0,68
1115	-1,16	-0,57

1116	-0,75	-0,75
1117	-1,36	-1,36
1118	-0,43	-0,58
1119	-0,76	-0,24
1120	-0,20	0,22
1121	-0,58	-0,08
1122	0,09	0,01
1123	0,27	0,23
1124	-0,25	0,05
1125	-0,85	-0,66
1126	-0,09	-0,08
1127	-2,21	-1,37
1128	-1,37	-0,64
1129	-1,42	-0,27
1130	-2,36	-0,15
1131	-0,85	0,33
1132	-0,16	0,36
1133	-1,51	-0,31
1134	-0,91	0,06
1135	0,24	0,46
1136	-1,03	-0,18
1137	-0,63	0,15
1138	-0,79	0,46
1139	-1,18	0,80
1140	-0,86	0,33
1141	-0,77	0,32
1142	-1,17	-0,01
1143	-0,09	0,63
1144	-0,89	-0,17
1145	-0,48	0,62
1146	-0,78	0,32
1147	-0,19	0,14
1148	0,13	0,59
1149	0,21	0,85
1150	-0,05	0,89
1151	-0,20	-0,24
1152	0,34	0,25
1153	0,41	1,12
1154	0,28	0,46
1155	0,83	1,08
1156	0,49	1,00
1157	-0,33	0,57
1158	0,47	1,00
1159	0,32	1,23
1160	0,21	1,20
1161	1,50	1,52
1162	1,10	0,98
1163	0,44	0,42
1164	1,13	0,77
1165	1,05	1,02
1166	0,71	0,75
1167	0,92	0,84

1168	1,37	1,10
1169	-0,14	0,31
1170	0,60	1,01
1171	-0,38	-0,13
1172	0,90	0,23
1173	0,03	0,01
1174	0,19	-0,40
1175	1,08	0,61
1176	-0,05	0,35
1177	0,08	0,35
1178	0,51	0,12
1179	-0,24	0,05
1180	0,54	0,13
1181	-0,21	-0,26
1182	-0,48	-0,16
1183	0,25	0,20
1184	0,77	0,47
1185	0,73	0,47
1186	-0,09	0,16
1187	0,31	0,34
1188	0,64	0,45
1189	-0,39	0,07
1190	0,39	0,30
1191	-0,08	0,27
1192	-1,48	-0,38
1193	0,61	0,44
1194	-1,68	0,21
1195	0,35	0,89
1196	0,12	0,55
1197	-1,32	0,08
1198	0,37	1,01
1199	0,80	0,97
1200	0,17	0,79
1201	-0,13	0,78
1202	-0,80	0,55
1203	0,68	1,26
1204	0,59	1,04
1205	0,15	1,07
1206	-0,39	0,93
1207	-0,80	0,21
1208	-0,99	0,48
1209	0,44	0,86
1210	-0,48	0,59
1211	-0,10	0,92
1212	0,19	1,09
1213	-0,12	0,98
1214	-0,17	0,88
1215	-0,64	0,31
1216	0,21	0,76
1217	0,98	0,79
1218	0,04	0,38
1219	-0,06	0,54

1220	-0,58	0,52
1221	0,75	1,02
1222	0,00	0,60
1223	-0,12	0,26
1224	0,27	0,59
1225	-0,65	0,43
1226	-1,23	0,27
1227	1,27	1,03
1228	-1,22	0,07
1229	-0,75	0,03
1230	-1,85	-0,23
1231	-0,91	-0,02
1232	-1,85	-0,46
1233	-0,64	-0,20
1234	-0,34	0,07
1235	-0,42	-0,04
1236	-0,67	-0,38
1237	-0,23	-0,30
1238	-1,54	-0,45
1239	-0,57	-0,15
1240	-0,57	0,05
1241	-0,59	0,06
1242	-0,82	-0,26
1243	-0,67	-0,08
1244	-1,26	-0,21
1245	-0,66	0,12
1246	-1,37	0,05
1247	-1,24	0,14
1248	-1,40	-0,26
1249	-0,99	-0,08
1250	-0,59	0,18
1251	-1,38	-0,16
1252	-1,83	-0,64
1253	-0,48	0,24
1254	-1,07	-0,43
1255	-0,83	-0,06
1256	-0,88	-0,40
1257	0,06	-0,07
1258	-1,37	-1,17
1259	-1,53	-0,70
1260	-1,54	-0,86
1261	-1,21	-0,68
1262	-1,51	-0,35
1263	-1,55	-0,49
1264	-1,90	-0,98
1265	-1,13	-0,44
1266	-1,10	-0,60
1267	-1,26	-0,77
1268	-0,61	-0,49
1269	0,56	0,26
1270	-0,21	-0,12
1271	-0,02	0,15

1272	-0,07	0,21
1273	-0,44	0,02
1274	-1,49	-0,50
1275	-1,04	-0,78
1276	-1,28	-0,76
1277	-1,68	-0,64
1278	-1,31	-0,30
1279	-1,17	-0,16
1280	-0,71	-0,21
1281	-1,30	-0,64
1282	-1,49	-0,82
1283	-0,57	-0,43
1284	-0,53	-0,03
1285	-0,18	0,29
1286	-0,48	0,14
1287	-0,19	-0,16
1288	-0,55	-0,01
1289	-0,47	-0,12
1290	-0,99	-0,76
1291	-0,69	-0,20
1292	-1,14	-0,48
1293	-1,06	-0,73
1294	-1,76	-1,15
1295	-0,14	-0,06
1296	-1,58	-0,52
1297	-0,51	0,21
1298	-0,81	-0,18
1299	-0,38	-0,13
1300	0,24	0,35
1301	-1,11	-0,55
1302	-0,30	-0,44
1303	-0,60	-0,51
1304	-1,03	-0,49
1305	-0,78	-0,71
1306	-0,15	-0,04
1307	-1,00	-0,69
1308	-1,13	-0,52
1309	-2,36	-1,39
1310	-0,08	-0,28
1311	-0,43	-0,14
1312	-0,40	-0,07
1313	-1,20	-0,55
1314	-1,21	-0,69
1315	0,38	-0,20
1316	0,75	0,07
1317	-1,08	-0,78
1318	0,18	-0,10
1319	-0,67	-0,75
1320	-0,08	-0,47
1321	-1,08	-0,41
1322	-0,69	-0,34
1323	-1,32	-0,68

1324	-0,94	-0,41
1325	-0,42	0,07
1326	-0,66	-0,54
1327	0,08	-0,34
1328	-1,44	-0,30
1329	-1,25	-0,85
1330	-1,48	-1,05
1331	-0,11	-0,57
1332	-0,95	0,07
1333	-1,48	-0,10
1334	0,43	0,64
1335	-0,46	-0,32
1336	-0,83	-0,32
1337	-1,17	-0,53
1338	-0,71	-0,48
1339	-0,92	-0,67
1340	-0,52	-0,36
1341	-1,50	-0,95
1342	-0,59	-0,48
1343	-0,14	-0,23
1344	-0,75	-0,31
1345	-1,11	-0,73
1346	-2,21	-1,43
1347	-0,60	-0,50
1348	-1,94	-1,13
1349	-2,19	-0,89
1350	-1,23	-0,84
1351	-0,06	-0,01
1352	-1,00	-0,66
1353	-1,05	-0,65
1354	-0,01	0,10
1355	-0,85	-0,51
1356	-0,86	-0,63
1357	-0,88	-0,48
1358	-1,33	-0,77
1359	-0,72	-0,54
1360	-1,04	-0,99
1361	-0,74	-0,40
1362	-0,70	-0,30
1363	-2,17	-0,47
1364	0,25	0,60
1365	0,31	0,44
1366	0,34	-0,09
1367	-1,04	-0,41
1368	0,38	0,01
1369	-0,78	-0,48
1370	-0,97	-0,61
1371	0,36	0,25
1372	0,67	0,15
1373	-0,84	-0,44
1374	0,23	0,14
1375	-1,23	-0,50

1376	-0,68	-0,59
1377	-1,63	-1,35
1378	-1,29	-0,76
1379	-0,23	0,18
1380	-0,58	0,08
1381	-0,11	0,14
1382	-0,38	-0,27
1383	0,68	0,71
1384	0,15	0,59
1385	-1,41	-0,18
1386	-0,13	0,54
1387	-0,38	-0,20
1388	-0,68	-0,32
1389	-1,19	-0,32
1390	-0,44	0,15
1391	0,00	0,15
1392	-0,86	-0,58
1393	-1,16	-0,21
1394	-1,74	-0,73
1395	-1,13	-0,32
1396	-0,59	-0,20
1397	-1,02	-0,31
1398	-0,90	-0,41
1399	-0,63	-0,40
1400	-0,95	-0,22
1401	-0,07	0,30
1402	0,40	0,71
1403	-0,24	0,44
1404	0,43	0,33
1405	-0,28	-0,11
1406	0,49	0,17
1407	0,07	0,06
1408	-0,13	-0,06
1409	0,07	0,36
1410	0,05	0,03
1411	1,25	0,55
1412	-0,63	-0,23
1413	0,47	0,36
1414	-0,62	-0,33
1415	0,32	0,15
1416	0,03	-0,23
1417	-0,63	-0,30
1418	0,14	0,30
1419	-0,57	-0,43
1420	-0,45	-0,11
1421	0,02	-0,05
1422	-0,60	-0,16
1423	-0,59	-0,51
1424	0,71	0,42
1425	0,68	0,27
1426	-0,04	-0,42
1427	0,49	-0,03

1428	-0,23	-0,45
1429	0,49	0,06
1430	-0,41	-0,33
1431	0,30	0,31
1432	0,64	0,24
1433	0,30	0,15
1434	0,97	0,40
1435	0,81	0,18
1436	0,04	0,06
1437	0,05	0,04
1438	-0,76	-0,17
1439	-0,83	-0,26
1440	-0,96	-0,22
1441	-0,15	0,05
1442	-0,74	-0,11
1443	-0,86	-0,31
1444	-0,62	0,06
1445	-0,40	0,06
1446	-0,74	-0,27
1447	-0,83	-0,07
1448	-0,30	-0,02
1449	-0,34	-0,08
1450	0,56	0,04
1451	0,04	-0,14
1452	-0,29	-0,14
1453	-3,06	-1,62
1454	-1,17	-0,81
1455	-1,63	-1,20
1456	-1,62	-1,29
1457	-1,50	-0,69
1458	-1,57	-0,67
1459	-1,45	-1,20
1460	-1,19	-0,77
1461	-1,73	-0,96
1462	-1,76	-0,98
1463	-1,95	-1,07
1464	-1,40	-0,69
1465	-0,85	-0,75
1466	-1,29	-0,61
1467	-1,10	-0,55
1468	-0,46	-0,62
1469	-0,75	-0,90
1470	-0,34	-0,81
1471	-0,78	-0,49
1472	-1,14	-0,59
1473	-1,53	-0,39
1474	-0,64	-0,17
1475	-0,91	-0,24
1476	-1,37	-0,11
1477	-0,91	-0,30
1478	-1,64	-0,62
1479	-0,35	0,03

1480	-0,83	-0,30
1481	-0,43	-0,21
1482	-0,49	0,00
1483	-1,21	0,02
1484	-0,06	0,43
1485	0,67	0,19
1486	-0,52	0,24
1487	-0,56	0,19
1488	-0,85	-0,18
1489	-0,42	0,05
1490	0,32	0,38
1491	0,10	-0,10
1492	0,47	0,26
1493	-0,51	-0,15
1494	0,49	0,48
1495	-0,26	-0,08
1496	0,65	0,18
1497	-1,95	-1,47
1498	-0,83	-0,81
1499	-0,50	-0,27
1500	-0,28	-0,02
1501	-0,46	-0,67
1502	0,26	0,97
1503	0,15	0,95
1504	-0,12	0,85
1505	0,30	-0,32
1506	0,42	0,22
1507	-1,61	-0,89
1508	0,34	-0,07
1509	-0,37	0,59
1510	-0,68	-0,45
1511	-0,31	-0,89
1512	-0,32	0,19
1513	-0,01	-0,38
1514	-0,67	-0,44
1515	0,05	-0,74
1516	-1,04	0,46
1517	-0,75	-0,04
1518	-0,12	-0,33
1519	-0,52	-0,25
1520	-1,25	-0,29
1521	-0,48	-0,16
1522	-0,92	-0,55
1523	-1,10	-0,51
1524	-1,76	-0,76
1525	-0,87	-0,09
1526	-1,12	-0,47
1527	-0,86	-0,74
1528	-0,93	-0,63
1529	-0,67	-1,44
1530	-0,89	-0,34
1531	-0,55	-0,43

1532	0,53	0,32
1533	0,59	-0,08
1534	0,47	1,22
1535	-0,49	0,56
1536	-0,30	1,08
1537	0,32	-0,29
1538	0,53	0,37
1539	0,22	0,25
1540	0,22	1,52
1541	0,01	-0,28
1542	-1,03	-1,63
1543	-0,66	-0,72
1544	-1,19	-0,74
1545	0,94	0,93
1546	-0,43	-0,10
1547	-0,18	-0,06
1548	-0,34	0,37
1549	-0,72	-0,54
1550	-1,15	-0,67
1551	-0,21	-0,05
1552	-0,34	-0,23
1553	-0,21	-0,16
1554	-0,50	-0,41
1555	-0,70	-0,93
1556	-0,15	1,09
1557	-0,81	0,13
1558	1,11	0,82
1559	-0,10	0,81
1560	-0,56	-0,53
1561	0,50	0,57
1562	-0,61	-0,31
1563	0,30	-0,77
1564	1,14	0,21
1565	0,53	0,50
1566	-0,13	0,15
1567	-1,26	0,12
1568	-0,56	-0,31
1569	0,35	-0,93
1570	-0,46	-0,73
1571	-0,41	-0,63
1572	-0,07	-0,11
1573	-0,99	-1,18
1574	-0,56	-0,29
1575	0,10	0,54
1576	-0,62	-1,23
1577	-0,60	-0,95
1578	-0,67	-0,51
1579	-1,33	-2,19
1580	-1,47	-0,75
1581	-0,82	-0,35
1582	-0,30	-0,43
1583	-0,02	0,08

1584	-0,68	-0,52
1585	-0,55	-1,37
1586	0,26	-0,10
1587	-1,82	-1,83
1588	-0,38	-1,56
1589	-1,38	-1,23
1590	-0,63	0,60
1591	-0,78	-0,97
1592	-0,64	-1,09
1593	-0,94	-1,62
1594	-1,06	-1,71
1595	-1,20	-1,66
1596	-1,48	-2,08
1597	-0,97	-1,47
1598	0,25	-0,74
1599	0,13	0,12
1600	-0,83	-1,47
1601	-2,48	-2,28
1602	-1,16	-1,14
1603	-0,97	-0,18
1604	-1,61	-0,67
1605	-1,59	-0,72
1606	-1,92	-1,62
1607	-2,03	-0,80
1608	-2,35	-1,93
1609	-1,85	-1,25
1610	-1,04	-0,05
1611	-0,97	0,06
1612	-0,99	-0,39
1613	-0,25	-0,21
1614	-2,55	-1,29
1615	-1,49	0,07
1616	-1,09	0,76
1617	-0,30	-0,66
1618	-1,38	-1,51
1619	0,13	-0,39
1620	-0,88	-0,48
1621	-0,64	-1,48
1622	0,33	-0,02
1623	-0,06	0,44
1624	0,00	0,32
1625	-0,96	-0,78
1626	0,35	-0,58
1627	0,10	-1,45
1628	-0,04	-1,83
1629	0,95	0,50
1630	-0,37	0,07
1631	0,57	0,61
1632	-2,12	-1,54
1633	-2,69	-1,84
1634	-0,29	-0,34
1635	-1,28	-0,93

1636	-0,22	-0,44
1637	-0,77	0,02
1638	-1,79	-0,29
1639	-0,91	-1,61
1640	0,51	-0,33
1641	-2,33	-1,68
1642	-0,92	-0,80
1643	-1,85	-0,67
1644	-0,91	-0,11
1645	-1,00	0,12
1646	-0,71	0,18
1647	-2,15	-1,28
1648	-0,08	-1,07
1649	0,22	-0,17
1650	-0,19	0,07
1651	-0,03	-0,03
1652	0,27	0,09
1653	-1,06	-0,63
1654	-0,68	-0,64
1655	0,57	0,17
1656	-0,21	-0,36
1657	0,03	-0,58
1658	0,27	-0,57
1659	-0,14	-0,51
1660	0,14	-0,20
1661	-0,07	-0,16
1662	-0,98	-1,10
1663	-1,50	-1,93
1664	0,53	-0,05
1665	0,57	0,23
1666	-0,09	0,97
1667	-1,44	-1,02
1668	-0,80	-0,33
1669	-0,99	0,72
1670	-0,84	-0,21
1671	0,03	0,21
1672	-1,32	-0,91
1673	-1,34	-1,04
1674	-1,36	-1,09
1675	-2,10	-2,18
1676	-0,40	-0,21
1677	-0,45	-1,10
1678	-0,41	-0,02
1679	-0,79	-0,50
1680	-0,85	0,01
1681	-0,38	-0,01
1682	-1,09	-0,97
1683	-0,19	0,05
1684	0,28	1,11
1685	-0,91	-1,60
1686	-1,21	-0,65
1687	-1,47	-0,73

1688	-1,23	-1,00
1689	0,86	-0,49
1690	-0,38	-0,76
1691	-0,13	-0,41
1692	0,13	-1,26
1693	0,55	0,18
1694	-0,40	-0,75
1695	-1,87	-1,95
1696	-1,42	-1,25
1697	-1,43	-1,27
1698	-0,28	-1,47
1699	-0,92	-0,83
1700	-0,12	-0,48
1701	-1,13	-0,62
1702	0,10	-0,43
1703	1,29	-0,27
1704	-0,91	-0,50
1705	-1,86	-0,64
1706	-1,61	0,06
1707	0,09	0,08
1708	-2,13	-1,42
1709	-1,75	-1,29
1710	-1,36	-0,99
1711	0,08	-0,25
1712	-0,52	-0,46
1713	-0,44	-1,25
1714	-0,30	-1,16
1715	0,23	-0,27
1716	-1,10	-1,41
1717	-0,94	-0,85
1718	-1,05	0,46
1719	-1,26	0,64
1720	-1,61	-1,17
1721	-0,81	-0,81
1722	-1,00	-0,84
1723	-0,77	-0,31
1724	-0,68	0,42
1725	-0,55	-1,51
1726	0,00	0,66
1727	-0,07	0,67
1728	-1,54	0,39
1729	-0,75	-0,02
1730	-0,06	-0,14
1731	-1,00	-0,49
1732	-0,26	-0,87
1733	-0,97	-0,55
1734	-0,87	-0,68
1735	-0,46	-0,29
1736	0,58	0,18
1737	-0,88	-0,78
1738	0,25	-0,01
1739	-1,03	-0,71

1740	-0,93	-1,44
1741	-1,75	-1,70
1742	-1,83	-1,33
1743	-1,19	-0,90
1744	-0,31	-0,25
1745	-0,61	0,15
1746	-0,20	0,59
1747	-0,79	0,08
1748	-0,66	0,38
1749	-0,31	-0,32
1750	-0,43	-0,30
1751	-0,27	-0,45
1752	0,58	0,23
1753	-0,37	-0,42
1754	0,04	-0,17
1755	0,29	-0,09
1756	-0,76	-0,50
1757	0,71	0,50
1758	-0,10	-0,73
1759	-0,14	-0,17
1760	0,48	-0,22
1761	1,20	0,42
1762	0,00	-0,02
1763	-0,03	0,14
1764	-0,47	-0,39
1765	-0,61	-0,55
1766	0,69	0,23
1767	-0,30	-0,18
1768	-1,17	-0,49
1769	-1,14	-0,59
1770	-0,57	-0,86
1771	-1,08	-0,98
1772	-1,99	-0,64
1773	0,08	-0,59
1774	-0,02	-0,11
1775	0,79	0,65
1776	1,08	0,12
1777	-0,67	-0,63
1778	0,04	0,28
1779	0,30	-0,34
1780	0,02	0,07
1781	-0,43	0,35
1782	-0,79	-0,09
1783	-1,28	-0,49
1784	-1,25	-0,90
1785	-1,18	-1,58
1786	-1,07	-1,62
1787	-1,55	-0,77
1788	-0,36	-0,10
1789	0,17	-0,73
1790	-2,14	-1,08
1791	-0,63	-0,17

1792	-0,90	-0,25
1793	-0,53	-0,08
1794	-0,25	0,19
1795	-0,68	-0,50
1796	-0,38	-0,23
1797	-0,55	0,22
1798	0,01	0,48
1799	-0,43	-0,69
1800	-1,24	-0,68
1801	-0,67	-0,71
1802	-1,29	-0,08
1803	-0,55	-0,13
1804	0,46	-0,05
1805	-0,81	-1,22
1806	-0,72	-0,60
1807	-0,40	0,90
1808	-0,14	0,12
1809	-0,86	-0,58
1810	-1,38	-1,03
1811	-0,48	0,34
1812	-2,26	-1,55
1813	-0,83	-1,77
1814	-0,47	-1,07
1815	-0,92	-1,76
1816	-1,23	-2,46
1817	-0,90	-1,07
1818	-0,73	-0,89
1819	0,77	-0,10
1820	-0,17	-0,71
1821	-2,41	-2,10
1822	-0,41	0,23
1823	-0,08	-0,65
1824	-0,38	-0,61
1825	-0,93	-0,62
1826	1,19	1,02
1827	-0,01	0,18
1828	0,18	0,05
1829	-0,58	-1,03
1830	-0,45	-0,22
1831	1,65	0,16
1832	-0,82	-0,75
1833	-1,18	-1,29
1834	-0,07	1,14
1835	-0,76	-0,17
1836	-1,25	-0,59
1837	-1,00	-0,40
1838	-1,54	-1,42
1839	-1,29	-0,53
1840	-0,95	-1,16
1841	-1,15	-1,38
1842	0,04	0,19
1843	-0,72	-1,51

1844	0,14	-1,14
1845	0,09	-0,59
1846	0,71	0,95
1847	0,46	-0,52
1848	-0,63	-0,42
1849	-1,09	-0,59
1850	0,24	0,07
1851	-0,94	-0,67
1852	0,66	1,35
1853	0,31	0,45
1854	1,48	0,29
1855	0,61	0,36
1856	-2,11	-0,85
1857	-0,69	1,06
1858	1,31	1,34
1859	-0,71	1,67
1860	0,42	-0,39
1861	1,17	1,13
1862	-2,12	-0,87
1863	-0,60	-0,27
1864	-0,95	-1,11
1865	-1,11	-0,26
1866	-0,61	0,08
1867	-1,47	-0,80
1868	0,94	1,88
1869	-0,62	-0,92
1870	0,25	-0,16
1871	-0,98	-0,54
1872	0,35	0,34
1873	0,36	0,59
1874	-1,14	0,01
1875	-0,31	1,00
1876	0,66	0,74
1877	-1,50	0,26
1878	-0,88	-0,07
1879	-0,11	-0,35
1880	-0,41	0,54
1881	-1,48	-0,63
1882	0,62	-0,17
1883	0,26	-0,01
1884	-0,71	-0,26
1885	-1,26	-0,60
1886	0,65	-0,42
1887	-0,79	-0,24
1888	-1,27	-1,24
1889	0,03	0,53
1890	-0,52	-0,92
1891	-1,24	-0,56
1892	-2,12	-0,47
1893	-1,03	0,26
1894	0,86	-0,16
1895	-0,27	0,14

1896	0,81	0,70
1897	0,01	0,78
1898	-0,20	-0,64
1899	-1,25	-0,05
1900	-1,25	0,63
1901	1,63	1,03
1902	-2,72	-1,52
1903	-1,14	-0,63
1904	-1,78	-0,12
1905	-0,08	0,81
1906	-0,21	-0,03
1907	-1,12	-1,49
1908	-0,76	-0,01
1909	-0,78	-1,01
1910	-1,23	0,14
1911	-0,74	0,88
1912	0,12	0,18
1913	0,06	-0,77
1914	0,34	1,07
1915	-0,94	-0,41
1916	-0,53	-1,15
1917	0,95	1,31
1918	-0,99	-0,76
1919	0,36	-0,92
1920	0,04	-0,27
1921	-0,67	-0,12
1922	-0,06	-0,88
1923	-1,98	-1,33
1924	0,20	-0,62
1925	0,90	0,53
1926	0,01	0,14
1927	1,17	-0,07
1928	-2,03	-1,17
1929	-1,29	-0,73
1930	1,10	0,63
1931	-0,81	-0,55
1932	-0,04	0,65
1933	0,66	0,73
1934	0,85	0,65
1935	-0,19	0,68
1936	1,75	0,80
1937	2,48	1,06
1938	1,40	0,56
1939	1,15	0,99
1940	0,27	0,15
1941	0,55	0,57
1942	-0,42	-0,34
1943	0,29	0,29
1944	-0,22	0,87
1945	0,96	0,72
1946	0,53	0,18
1947	1,22	1,73

1948	-0,31	0,21
1949	-1,05	-0,09
1950	0,40	0,80
1951	-0,31	0,19
1952	-0,77	-0,17
1953	1,12	0,82
1954	0,06	-0,40
1955	-0,05	0,64
1956	-0,67	-1,00
1957	-0,06	0,13
1958	-0,74	-0,27
1959	0,79	1,37
1960	1,38	-0,13
1961	0,77	-0,43
1962	-1,97	-1,48
1963	-0,28	0,34
1964	-0,61	-0,11
1965	-1,09	-1,08
1966	0,56	0,14
1967	0,13	0,16
1968	-0,34	0,42
1969	0,69	0,89
1970	1,22	0,33
1971	-0,19	0,13
1972	2,14	0,30
1973	1,48	0,78
1974	0,45	-0,60
1975	-0,68	1,16
1976	-0,75	0,72
1977	-0,81	-0,43
1978	-0,69	-0,62
1979	0,59	-0,47
1980	1,04	-0,22
1981	-0,94	-0,43
1982	-0,79	0,82
1983	-0,10	1,04
1984	-0,41	-0,41
1985	0,12	-0,53
1986	0,20	-0,18
1987	-1,68	-1,30
1988	1,39	0,39
1989	0,59	0,37
1990	0,16	0,41
1991	0,24	0,26
1992	-0,21	1,70
1993	-1,11	-0,90
1994	0,57	1,44
1995	0,35	1,10
1996	0,09	0,00
1997	1,93	1,89
1998	-0,41	-0,47
1999	0,85	0,88

2000	0,21	-0,10
2001	0,99	0,72
2002	2,14	2,06
2003	1,06	2,07
2004	0,36	0,43
2005	1,28	0,49
2006	1,64	2,08
2007	0,80	1,04
2008	-0,60	1,18
2009	0,33	0,84
2010	1,00	1,43
2011	0,17	0,51